RSC Advances

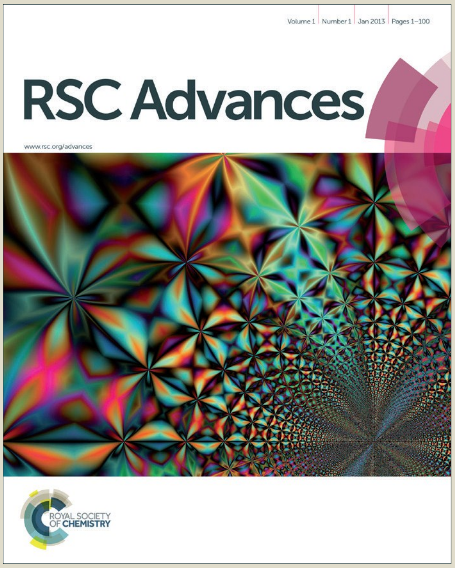

ROYAL SOCIETY OF CHEMISTRY

www.rsc.org/advances

Colour graphic:

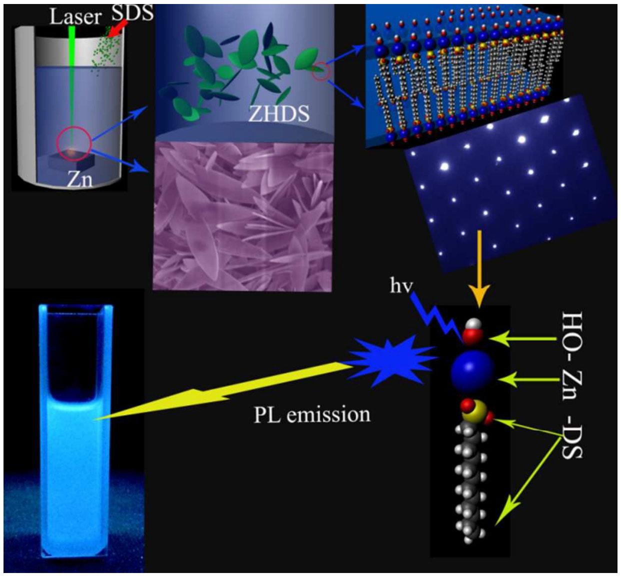

TEXT : The successful synthesis of single crystal zinc hydroxyl dodecylsulfate nano-sheets with excellent photoluminescence emission by laser ablation in liquid

Laser-induced fabrication of single crystal zinc hydroxyl dodecylsulfate nano-sheets with excellent fluorescence emission

Shuang Li, DaMeng Wang, ZiYu Wang, ZiWei Wang, Ming Chen[*] and XiangDong Liu

School of Physics, Shandong University, Jinan250100, China

[*]chenming@sdu.edu.cn

Abstract:

An attractive strategy to convenient synthesis of free-standing single-crystal zinc hydroxyl dodecylsulfate (ZHDS) nano-sheets has been developed by simple using laser ablation of bulk Zn metal target in liquid medium containing deionized water and enough/excess sodium dodecylsufate(SDS). Taking advantage of enough/excess amount of sodium dodecylsfulfate(SDS), a tightly packed and highly ordered layers of DS functional groups were generated and resulted the crystallization of metallo-organic ZHDS nano-sheets over the plasma created by laser ablation of Zn target. The experimental results confirm that the ZHDS nano-sheets are indeed softer materials and intercalated with numerous DS functional groups in crystal structures. The novel free-standing two-dimensional ZHDS nano-sheets exhibit excellent fluorescence emission at 417 nm. It has been proved that the hydroxyl (-OH) groups should play the main role for the outstanding photoluminescence in the blue-band region. Moreover, the strong blue emission can be changed to the bright green-band emission (vacancy oxygen-related PL emission in ZnO) centered at about 516 nm after annealing the ZHDS nano-sheets at 400^{o}C for 3 hours. The excellent performances will be great significance for ZHDS nano-sheets in low-cost metallo/organic light-emitting material and photo-electron-chemical bio-analysis in the future. Based on pulses laser fabrication in liquid, the new conjugation of metal complexes and organic compounds has opened up exciting classes of hybrid materials for applications spanning optoelectronics, energy conversion, and photodynamic therapy, etc.

Electronic Supplementary Information (ESI) available: EDS patterns of the typical productions with SDS concentrations of 0.5, 25, 50 mM, respectively. See DOI:10.1039/x0xx00000x

Introduction

As one of the novel free-standing two-dimensional (2D) nano-materials, single-crystal metallo/organic compound structure is characterized by a nano-scale dimension only in the *c* axis and infinite length in the plane, which is emerging as an exciting class of material that integrates the unique optical, electronic properties of metal complexes with the specificity and highly ordered structures of organic polymers.[1-5] Compared with organic dyes and polymers, the metallo/organic compounds are generally characterized by additional properties such as high thermal, optical stability and remarkable electron transport and excellent luminescent properties. Arising from their own suite of single crystal-like structural, enlarged surface area, unusual chemical and optical properties, the fascinating metallo/organic nano-objects have attracted tremendous attention in 2D nano-structures owing to their intriguing application potentials for super-active catalysts, low-cost organic light-emitting devices, and biomedical sensors, etc.[2-5] Increasing evidences have proven that the convenient synthesis of stable structures is of great significance for the specific applications, since the unique properties of the metallo/organic nano-materials are highly dependent on their free-standing 2D structures.

Typical approaches for preparing the nano-sheets mainly include the delamination of layer-structured materials by aqueous-phase,[6] solution-phase synthesis,[7-8] selective etching of sacrificial layers,[9-11] etc, which are generally suit for fabrication of only metal oxides and semiconductors such as GaAs, CdTe, CeO_2, Ceria, silicon, etc. It should be noted that the methods with low-cost and convention fabrication of metallo/ organic compounds are also sporadically. New strategy to synthesis of organic/inorganic hybrid nanocomposites need to be developed to obtained free-standing 2D functional materials. Recently, many interesting works[2-3] such as fabrication of metallo/ organic single crystalline zinc hydroxyl dodecylsufate (ZHDS) nanosheets have been reported by Wang *et al.* using a surfactant-directed assembly approach. It was suggested that the tightly packed DS ions can be formed by using enough amount SDS, resulting in the crystallization of single crystal metallo/organic nano-structures. Moreover, Koshizaki *et al.*[5] investigated layered $Zn(OH)_2$/ZnDS platelets by laser ablation in aqueous solution of SDS. Laser fabrication in solution as a new green approach for synthesis of novel nano-materials represents an interesting technique with high-temperature and pressure feature.[5,12-14] Inspired by these previous works[2,3,5], in this paper we report the successful synthesis of ZHDS single crystal-like 2D nano-sheets via simply using laser ablation of bulk Zn metal target in solution containing enough/excess (>25mM) amount of SDS as templates and very few hydrogen chloride (HCl, ~0.01mM). In our synthesis, the few hydrogen chloride used in this paper plays an important role for improving SDS hydrolyzing degree in liquid and will enable $Zn(OH)_2$ to dissolve and remove from final products, which is the main difference from the experiments in recent works.[2,3,5] Moreover, it was confirmed that the ZHDS nano-sheets obtained in this paper are indeed softer material and intercalated with some DS groups in the crystal structures. The metallo/ organic ZHDS nano-sheets show strong fluorescence emission at 417 nm. The enhanced blue-band emission can be changed to the green-band emission (vacancy oxygen-related PL emission in ZnO) centered at about 516 nm after annealing the ZHDS nano-sheets at 400°C for 3 hours. Meanwhile, a discussion of fluorescence mechanisms based on zinc-hydroxyl functional groups has been addressed. Our results prove a new conjugation of metal complexes and biopolymers by coupling laser ablation technique with enough/excess surfactant as templates, which is a green, low-cost and convenient synthesis technique possessing great potential in fabrication of various metallo/ organic compounds in the future.

Experimental setup

In a typical experiment, a well polished pure (99.99%) Zn target was placed on the bottom of a rotating glass dish with speed of ~200 rpm filled with ~3.5mm depth of SDS solution with concentrations of 0.5mM~50mM. A Q-switched Nd-YAG(Yttrium Aluminum Garnet) laser (Quanta Ray, Spectra Physics) beam operating at wavelength of 1064 nm with a pulse duration of 10 ns and 10Hz repetition rate was focused onto the Zn metal surface. The laser beam was focused onto the Zn target by a quartz lens with 40 mm focal length, and the average spot size of the laser beam at the target was measured to be about 350 μm. The laser beam intensity was about 6 GW/cm^2, and the ablation lasted for 1 hour. After laser fragmentation, the nano-particles were repeatedly centrifuged at 2000 rpm for 15 min by an ultracentrifuge, and the precipitates were carefully washed in ethanol three times. A 325 nm cw semiconductor laser with power of 18mW was used as an excitation source, and the photoluminescence spectrums of the colloidal suspensions were dispersed by a monochromator (Jobin-Yven iHR320) with a 300n/mm grating, and detected by a coupled with a thermoelectrical cooled Synapse CCD detector. The sediments were dropped on a copper mesh and dried in oven at room temperature for observation by transmission electron microscopy (JEOL-JEM-2100F). Additionally, the crystallographic investigations of the nano-materials were analyzed by X-ray diffraction (XRD) patterns (Rigaku RINT-2500VHF) using Cu Kα radiation (λ = 0.15406nm). Morphological images and chemical compositions were measured by field emission scanning electron microscope (SEM, Hitachi S-4800) equipped with energy-dispersive x-ray spectroscopy (EDS). The Fourier transforms infrared spectrums (FT-IR) of the ZHDS sediments were measured by a UV-Vis-NIR spectrometer (Shimadzu, UV-1700).

Results and discussion

After multiple pulses laser ablation of Zn metal in solution with the SDS concentration of 0.5mM, the typical low-magnification SEM and TEM images of the nano-particles were shown in Fig.1(a1-a2), respectively. The morphologies clearly show that numerous quasi-spherical nano-particles with the diameter varying from about 140 nm to 210 nm are likely fabricated one by one separately, and almost not joint together. The result of EDS in Fig.S1(a) demonstrates that the nano-particles are composed of Zinc and Oxygen elements (Si signal from Si substrate). The ratio of Zn and O is calculated about 4:3. Moreover, the HRTEM image in the inset of Fig.1(a2) provides the structural detail of the representative nano-particles. The periodicity corresponding to a d-spacing of 0.262 nm could be indexed as (002) plane in the wurtzite ZnO structure. It is reasonable to deduce that the SDS surfactant with low density acted as a dispersing agent plays a critical in the formation of mono-dispersed ZnO nano-spheres. On the other hand, $Zn(OH)_2$ materials[5,13] were dissolved and removed from nano-structures due to the reaction by the acid solution. Further increasing the SDS concentration to 25 mM, a highly ordered monolayer of DS ions was obtained and enabled ZHDS nano-membranes to form in the liquid after laser ablation of Zn target, as the SEM and TEM images shown in Fig. 1(b1-b2). The typical SEM morphology shows that numerous ZHDS nano-membranes in the size of ~1.2 μm are quasi- hexagonal like multiple layers with smooth surfaces and non-uniformity in thickness. Furthermore, the EDS pattern in Fig.S1(b) illustrates that signals from S, Zn, O, C can be all clearly detected, and the measured ratio of them is about 0.8: 0.8: 3.2: 5.2, respectively. The ratio of Zn, S to O is completely fit to stoichiometry of ZHDS component, supporting the formation of ZHDS nano-membranes instead of $Zn(DS)_2$ structure. Meanwhile, it is necessary to note that the measured ratio of C element in EDS pattern is some lower than the ZHDS structures, implying the DS functional groups should be vertical arrayed in the ZHDS crystal structures rather than accreted on the outer surfaces. TEM image in Fig.1(b2) illustrates that the ZHDS nano- membranes are actually composed of multiple layers plates, since the exposed layered-structures can be clearly observed at the boundary where the plates meet. As shown the inset of Fig.1(b2), the selected area electron diffraction (SAED) pattern taken from an individual ZHDS nano-membrane contains discrete bright and weak spots that can be fitted into hexagonal symmetry and orthorhombic super-lattice, which agree well with the detailed discussions in previous report.[2-3] Then, we increased the concentration of SDS to 50mM, and found that some more fascinating ZHDS nano-sheets with willow leaf- shaped structures were investigated by the SEM and TEM images, as displayed in Fig. 1(c1-c2). The typical short axis and long axis are calculated about 1.53 and 5.5μm, respectively. The willow leaf-shaped ZHDS nano-structures have some differences from the ZHDS nano-membranes fabricated with SDS of ~25mM. We deduce that the excess amount of SDS coupled with few acid solution enable the dense DS functional groups and hydroxy groups (-OH) to form quasi-ellipsoid shaped structures as templates. Laser induced Zn plasmas with high temperature and pressure will press the template flat, then conjunct with hydroxyl groups and DS ions, which is the reason for the closed leaf-like ZHDS nano-sheets obtained in this paper. The signals of S, Zn, O, C elements are also detected in the EDS pattern (Fig.S1(c)). Because of the obvious curved surface in the edge regions of willow leaf- shaped ZHDS nano-sheets, the ratio of C to Zn, S, or O is improved to about 8.3:0.8:0.8:3.2. The clearly spots in electron diffraction pattern (inset in Fig.1(c2)) sufficiently confirms that the single crystal ZHDS oblate spherical nano-sheets can be fabricated by laser ablation of Zn with excess amount of SDS. Compared with the electron diffraction pattern from ZHDS nano-membranes, the more regular spots in Fig.1(c2) suggest that the crystallization of ZHDS can be evolved into tetragonal symmetry as the structures changed to oblate sheets by adding excess amount of SDS. In addition, the crystallographic investigations of ZHDS nano- membranes and willow leaf-shaped sheets were established by X-ray diffraction (XRD) in Fig.1(d). The low-angle-XRD (10~20^o) patterns clearly reveal that a series of (001), (002), and (003) ZHDS diffraction peaks centered at 11.037^o, 13.240^o, and 17.691^o were indeed detected, and higher-order diffractions at higher angles(20^o~30^o), which agree well with the results obtained by Wang *et al.*[2,3] In order to further confirm the DS functional groups and hydroxy groups (-OH) crystallized in nano-products, the Fourier transforms infrared spectrums (FT-IR) were used to characterize the ZnO and willow leaf-shaped ZHDS sheets in Fig.1(e). FT-IR spectrum of ZnO nano-structures are characterized by very weak signals from organic material, which are possible originate from the few amount of SDS surfactants inevitably resided on ZnO materials after the products have been washed by ethanol. As for ZHDS nano-sheets, several improved FT-IR spectrums from organic material can be detected. The peaks located at 2957.39, 2918.98, 2850.97, 1655.71,1648.84, 1383.00 and 1221.86 cm^{-1}can be attributed to the C-H functional groups, and the peak located at 3465.84 cm^{-1} should be originated from the adsorption of the hydroxy groups (-OH), which are best evidences for the ZHDS compounds formed in this paper.

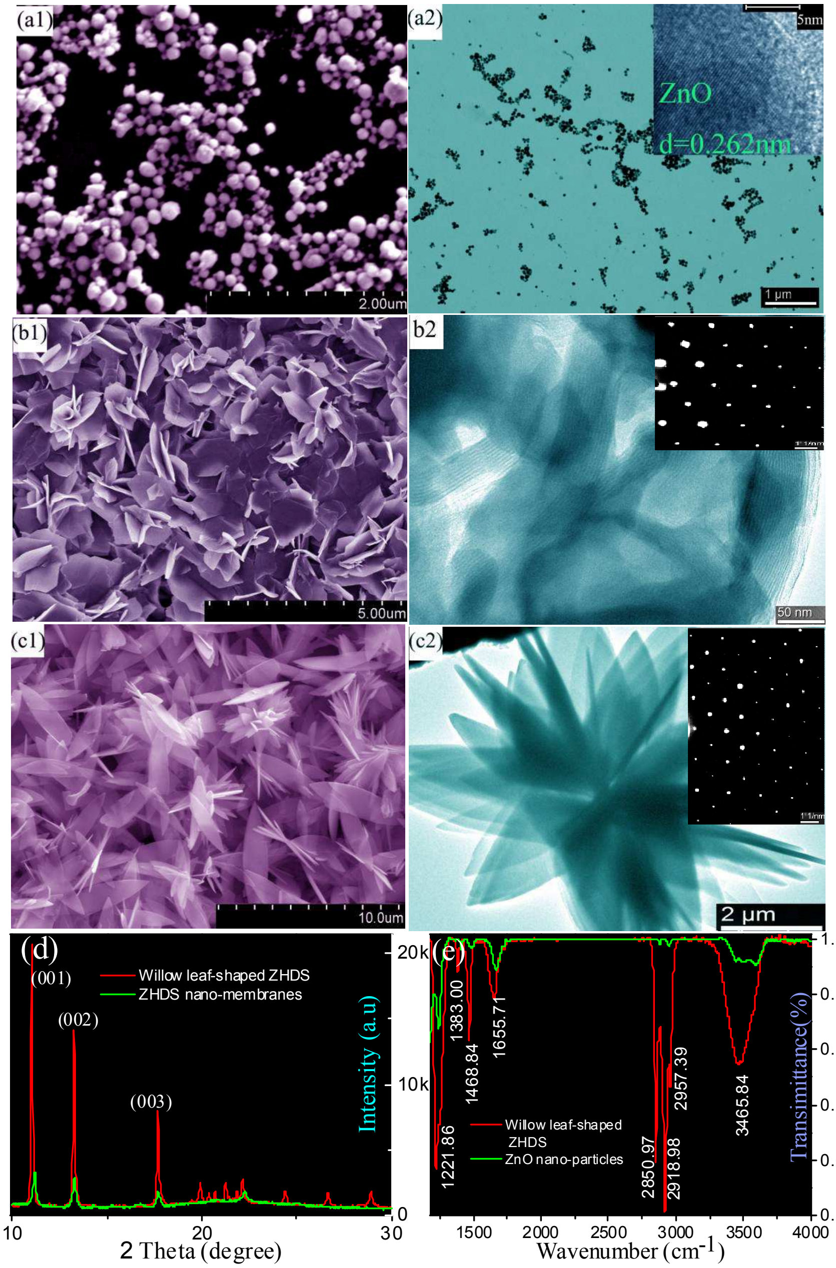

Fig. 1 Representative SEM and TEM images of the typical nano-structures by laser ablation of Zn target in liquid solution of SDS with different concentrations: (a1-a2) 0.5mM, (b1-b2) 25mM, (c1-c2) 50mM, respectively. Insets show the corresponding SADE patterns. (d,e) XRD and FT-IR spectra of the typical products with SDS concentrations of 25 and 50 mM, respectively.

The possible ZHDS nano-sheet growth processes have been proposed in the following section. Figure.2 provides a schematic growth diagram of ZnO nano-particles, ZHDS nano-membranes, and willow leaf-shaped ZHDS fabricated with different SDS surfactant concentrations of low (0.5mM), enough (25mM) and excess (50mM), respectively. In brief, the SDS with low concentration acted as dispersing agent will result in the formation of spherical-like ZnO nano-structures. The few hydrogen chlorides in solution will significantly improve the SDS hydrolyzing degrees:

$$CH_3\text{-}(CH_2)\ \text{–}CH_2O\text{-}SO_3Na + H_2O \rightarrow CH_3\text{-}(CH_2)\ \text{–}CH_2O\text{-}SO_2\text{-}OH + NaOH \qquad (1)$$

$$H^+ + OH^- \rightarrow H_2O \qquad (2)$$

On the other hand, enough concentrations of SDS surfactant can enable the DS and hydroxyl functional groups to form a tightly packed monolayer in the liquid. Moreover, the templates with quasi-ellipsoid shaped structures tend to be created for using of excess SDS surfactants in the liquid. As shown in Fig.2, the quasi-ellipsoid shaped template is characterized by a radial –like structure with the hydroxyl groups pointing outward and the hydrophobic DS functional groups arraying toward the core. The radial-like template is the most possible structure as the dense hydrophilic groups and hydrophobic groups huddled together in water. The higher ordered DS and –OH groups act as templates for the formation of nano-sheets. In the laser ablation (0~30ns) of Zn process, the superheating will play a critical role in the early stage, resulting in excited Zn ions with higher temperature and pressure rapid spreading in solution. During pulses laser-induced Zn plasmas in the liquid, the excited Zn ions can easily conjunct with DS and hydroxyl functional groups. Meanwhile, the templates will be pressed into flat-like structures owing to Zn plasmas characterized by high pressure property in liquid.[5,12-13] Considering the numerous templates in the liquid, the ZHDS nano-sheets will be obtained by charge-matching mechanism as follows[5]:

$$CH_3\text{-}(CH_2)\ \text{–}CH_2O\text{-}SO_2\text{-}OH + Zn \rightarrow CH_3\text{-}(CH_2)\ \text{–}CH_2O\text{-}SO_2\text{-}Zn\text{-}OH \qquad (3)$$

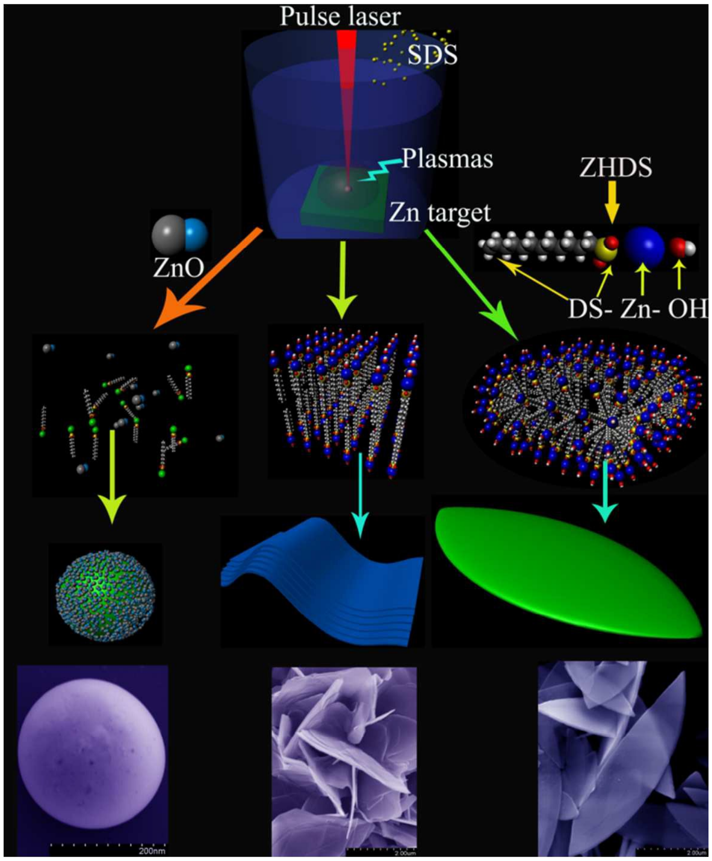

Fig. 2 The schematic growths of ZnO, ZHDS nano-membranes and willow leaf-shaped ZHDS fabricated by pulses laser ablation of Zn target in solution containing SDS with low (0.5mM), enough(25mM), and excess(50mM) concentrations, respectively.

The acid condition plays an important role for improving the SDS hydrolyzing degrees, which is the main reason for the fabrication of the pure ZHDS single crystalline nano-sheets. If the hydrogen chloride with low concentration (0.001mM) was used in this experiment, $ZnO/Zn(OH)_2$ hybrid byproducts will be also formed. As shown in Fig.3, in contrast to willow leaf-shaped ZHDS with smooth surfaces obtained in Fig.1, the ZHDS nano-sheets with rough surfaces are accreted with numerous of $ZnO/Zn(OH)_2$ hybrid nano-composites on the outsides. The $ZnO/Zn(OH)_2$/ZHDS compounds should be highly related to the fact that there are incompletely SDS hydrolyzing reactions, resulting in insufficient DS ions and –OH groups formed in liquid.

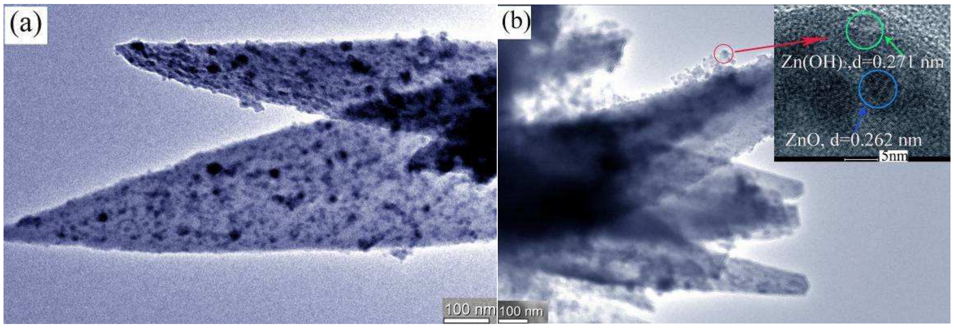

Fig.3 Laser ablation of Zn target in 50mM SDS solution with HCl concentration of 0.001mM.

The ZHDS nano-sheets were believed to be softer materials in previous reports,[2,3,5] and some DS functional groups will be incorporated in the crystal structures. To verify it, the willow leaf-like ZHDS nano-sheets were subjected to 15KeV and 80KeV electronic beams irradiated for one minute. Figure. 4(a, c) show the typical SEM and TEM images of the willow leaf-like ZHDS nano-sheets before electronic beams irradiations. After irradiation by 15KeV electron beam for one minute, many obvious bubbles formed in the subsurface of ZHDS nano-sheets, as shown in Fig. 4(b), which can be reasonably explained by using sub-surface micro-explosions boiling models. The interesting phenomenon confirms that many organic DS functional groups are indeed trapped and intercalated in the interiors of ZHDS nano-sheets structures. As for 80KeV electron beam used in Fig.4(d), several nano-holes with different sizes of 20 ~ 100 nm were formed in nano-sheet structures after electron beam got through the surface, arising from the fact that the hydrocarbon groups trapped in the interiors can be completely removed from nano-sheets. The ZHDS nano-sheets are indeed much softer, and behaved similar to the polymers structure, which will be very suitable for the fabrication of novel organic/inorganic porous nano-cages in the further.

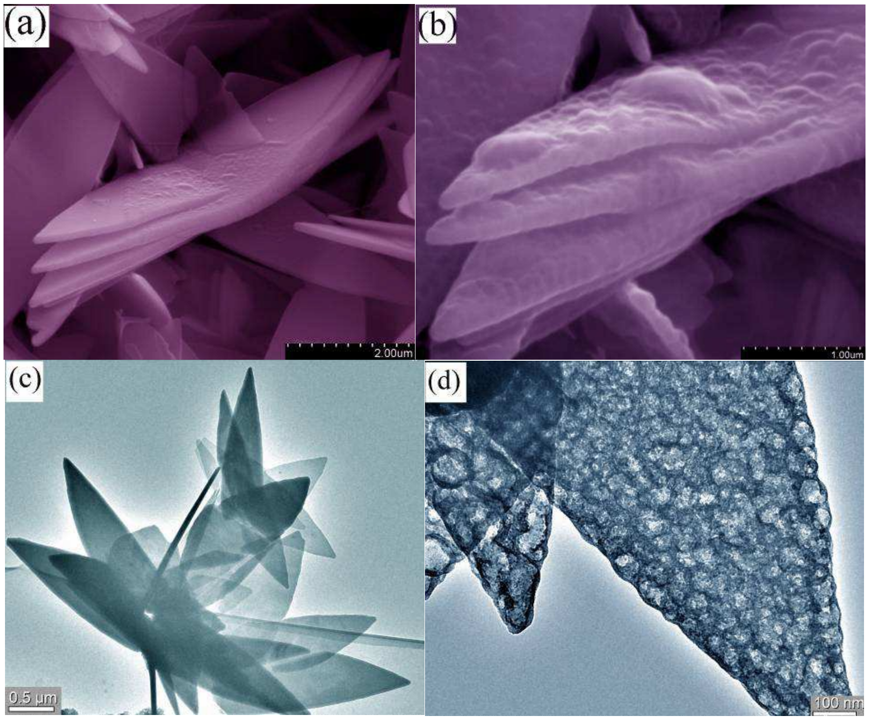

Fig. 4 (a, b)The typical SEM images of the willow leaf-like ZHDS nano-sheets before and after 15KeV electron beam irradiations for one minute, respectively. (c, d) The representative TEM images of the nano-sheets before and after 100KeV electron beam irradiated for one minute, respectively.

Finally, the unique optical properties of ZHDS single crystal nano-sheets were illustrated by photoluminescence spectra, some more fascinating and visible enhanced fluorescence blue-band emission at about 417 nm are illustrated in Fig.5(a). The PL spectrums of willow leaf-shaped ZHDS nano-sheets clearly reveal that the peak intensities at 417 nm drastically increased to about 63163 a.u, which is almost 2.7 times higher than that (~22825 a.u) obtained from ZHDS nano-membranes, and is nearly a fact of 15 higher than the result (~3998 a.u) originated from ZnO nano-spheres. The weak PL green-band emission of inorganic ZnO nano-spheres should be proposed with the vacancy oxgen(VO)-related emission in ZnO, which have been discussed by Liang *et al.*[15] Compared with the weak green-band emission of inorganic ZnO nano-spheres, it is surely that the metallo/organic ZHDS nano-sheets are characterized by strong blue-band emission, which can be also clearly confirmed by the corresponding direct photographs of the three colloidal suspensions under irradiation by a 254 nm UV lamp, respectively, as the insets shown in Fig.5(a). Moreover, the strong blue emission at 417 nm excited from ZHDS nano-sheets can be changed to the bright green-band emission (a very typical vacancy oxygen-related PL emission in ZnO) centered at about 516 nm after annealing them at 400^{o}C for 3 hours, as shown in Fig.5(b). The inset in Fig.5(b) clearly reveals that the blue-band emission at 417 nm and green emission at 516 nm separately drastically decrease (63000~28390 a.u) and improve (32826~67626 a.u) with the increase of the anneal temperature(100~400^{o}C). After annealing, the interesting result should be related to the fact that more ZnO nano-particles will be formed from hydrolysis of ZHDS nano-sheets. As for metallo/organic ZHDS nano-sheets, we deduce that the enhanced blue-band emission at about 417 nm should be highly related to Zn-OH groups. The inset in Fig.5(a) shows the schematic PL emission during a 352 nm cw laser irradiation on Zn-OH groups. Increasing evidences[16-20] have proven that numerous different sizes functional group such as –OH, –NH_2, –H, etc in metal/organic frame-structures are the main reasons for the obtained strong fluorescence emission. On the other hand, the highly ordered single crystal-like structures are also usually discussed in the areas of oxide semiconductors[21-24]. Then, which one can play a critical role for strong PL emission of ZHDS nano-sheets in this paper? The problem will be neatly solved in the following section.

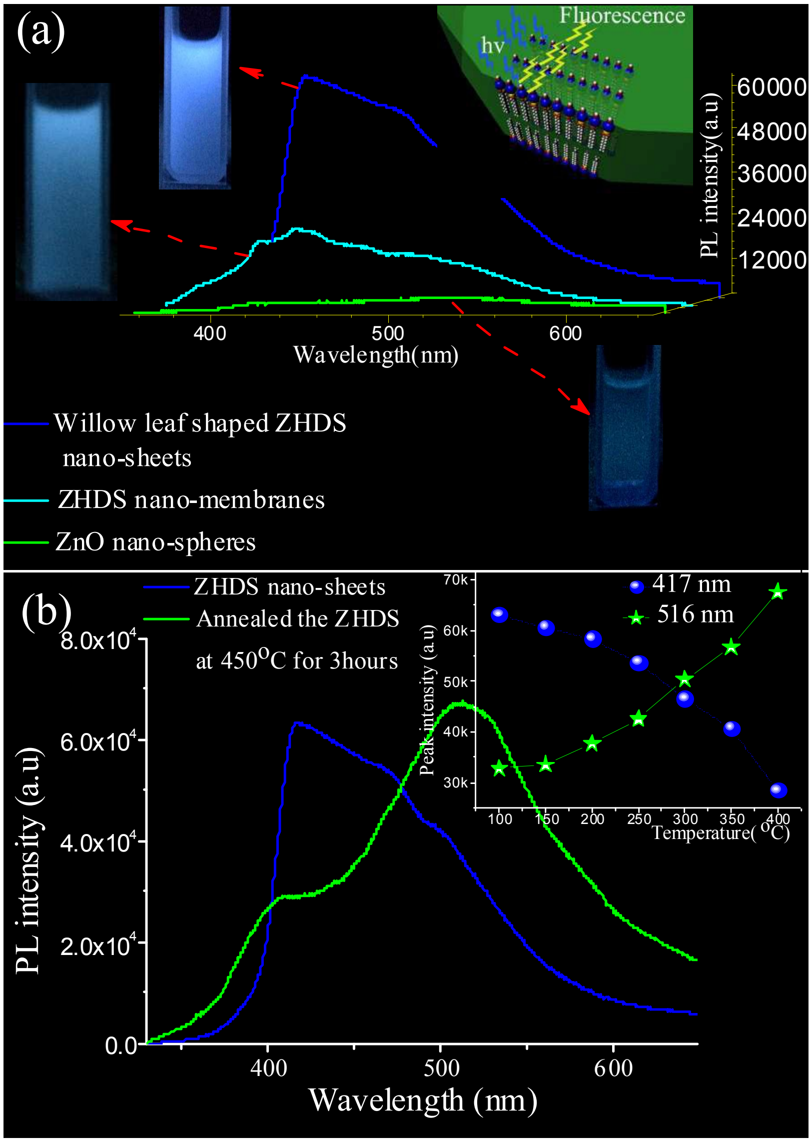

Fig. 5 (a)The photoluminescence (PL) spectrums of the ZnO nano-spheres, ZHDS nano-membranes, and willow leaf-like ZHDS nano-sheets, and the corresponding direct photographs of the three colloidal suspensions under irradiation by a 254 nm UV lamp, respectively. The up inset is the schematic PL emission during a 352 nm cw laser irradiation on ZHDS nano-sheets. (b) PL spectrums of willow leaf-like ZHDS nano-sheets before and after annealing them at 400°C for 3 hours. The inset shows the peak intensities of PL spectra at 417 and 516 nm *versus* different anneal temperature for 3 hours in vacuum condition.

It is well known that the hydroxy groups (-OH) are characterized by typical chemistry reducing property, which will be easily dissolved by adding some strong oxidant in liquid due to the oxidation-reduction reaction. Following this mechanism, the $HAuCl_4$ materials were added in willow leaf-shaped ZHDS nano-sheets liquid solution, resulting in a significant change of nano-structures, as the TEM images shown in Fig.6(a,b). By adding 20mL $HAuCl_4$ materials with concentration of ~40 mM into 300mL ZHDS nano-sheets solution(200mM), the morphologies of the final ZHDS/Au hybrid nano-composites changed to porous plate structures accreted with Au nano-particles on the surface. In addition, XRD pattern in low angle range ($10{\sim}20^o$) clearly reveals that the porous plate structures are also contain a series of (001), (002) and (003) diffraction peaks from ZHDS nano-sheets, as the overlap signals shown in Fig.6(c). Meanwhile, a series of (111), (200), and (220) single crystal Au nano-particles diffraction peaks separately centered at 38.194^o, 44.408^o and 64.518^o were also indeed detected in ZHDS/Au hybrid nano-composites. In order to further confirm the DS functional groups and hydroxy groups (-OH) existed in ZHDS/Au hybrid nano-composites, the FT-IR spectrums were investigated in Fig.6(d). The peaks in the range of 1000 ~3000 cm^{-1}can be attributed to the DS functional groups, which are nearly remain the same level for both ZHDS nano-sheets and ZHDS/Au hybrid nano-composites. However, the peak located at 3465.84 cm^{-1} originated from the hydroxy groups (-OH) drastically decrease as the ZHDS nano-sheets changed to ZHDS/Au hybrid nano-composites. Based on the results in Fig.6(a-d), it is reasonable to deduce that the $HAuCl_4$ materials should enable the ZHDS/Au hybrid nano-composites to sustain for single crystal nano-structure, and simply make the -OH groups to be removed from the nano-sheets. In this way, the lesser $HAuCl_4$ materials will make fewer -OH groups to be removed from the nano-sheets, resulting in a series of ZHDS/Au hybrid nano-composites with different amount of -OH groups. The peak intensities of PL blue-band emission at about 417 nm *versus* the $HAuCl_4$ concentration of 1.2 ~40 mM are displayed in Fig.6(e). It is noted that the peak intensities of PL spectrums significantly decrease from about 63000 to ~1600 a.u, as the $HAuCl_4$ concentration increased from ~1.2 to ~40 mM. The fluorescence reduction behavior can be confirmed by the direct photographs of strong and weak fluorescence emission from ZHDS/Au hybrid nano-composites irradiated by a 254 nm UV lamp under the conditions of ~1.2 and ~30 mM $HAuCl_4$ concentrations, respectively, as shown inset in Fig. 6(e). In summary, we confirm that the -OH groups play the main role for the strong blue-band emission of ZHDS nano-sheets in this paper. Furthermore, the ZHDS single crystal nano-sheets will be very suitable for developments of low-cost metallo/ organic light-emitting material and new hollow nano-particles owing to their excellent fluorescence emission and softer structures.

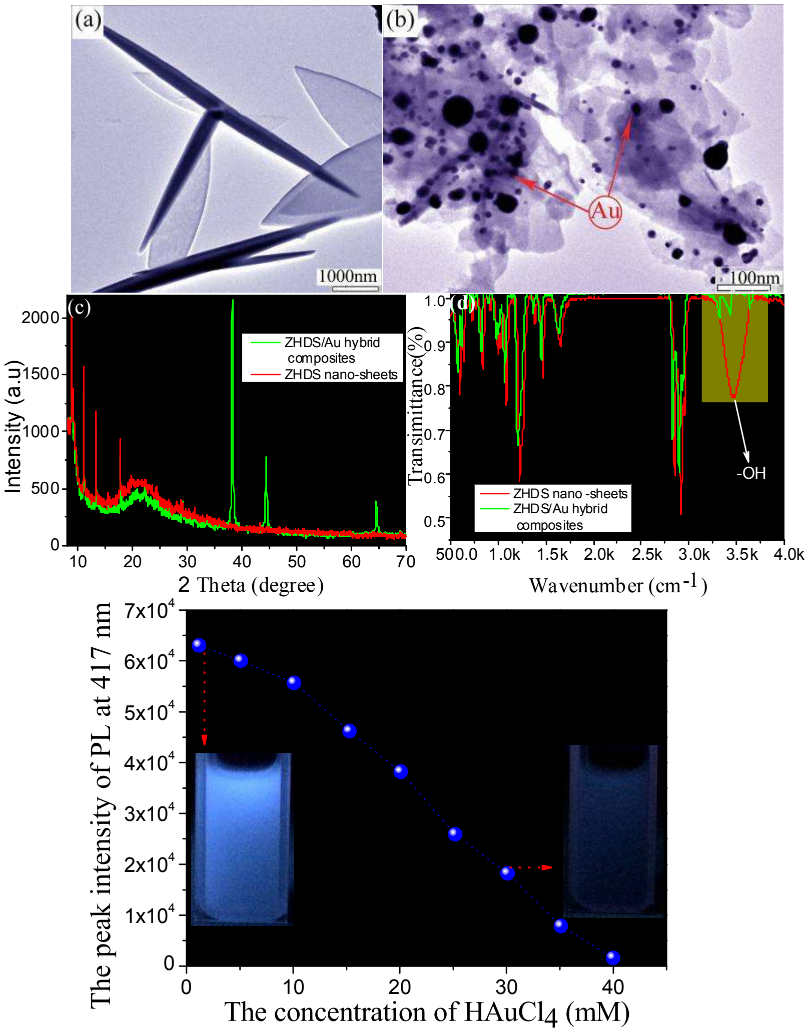

Fig. 6(a,b)TEM images of ZHDS before and after adding 40mM $HAuCl_4$ materials, respectively. (c,d) XRD and FITP spectrums of the ZHDS before and after adding 40mM $HAuCl_4$, respectively. (e) The peak intensities of PL spectrum of ZHDS/Au hybrid nano-composites at about 417 nm *versus* the $HAuCl_4$ concentration, and the insets are the photographs of the hybrid nano-composites irradiated by a 254 nm UV lamp under $HAuCl_4$ concentration of ~1.2 and 30mM, respectively.

Conclustions

In summary, free-standing ZHDS single crystal nano-sheets have been carefully devised through laser ablation of bulk Zn metal in liquid medium containing enough/excess SDS surfactants as templates and very few hydrogen chlorides. The enough (~25 mM) and excess (~50 mM) SDS concentrations used in this paper will enable the DS functional groups and –OH groups to aggregate into a tightly packed monolayer and quasi-ellipsoid shaped structure in liquid. The two different highly ordered templates will result in the formation of ZHDS nano-membranes and willow leaf-shaped ZHDS sheets, respectively. It was found that the ZHDS nano-sheets are indeed softer material, and the intercalated DS groups can be trapped in the crystal structure. The single crystal ZHDS nano-sheets show strong PL blue-band emission at about 417 nm. The enhanced blue-band emission can be changed to the bright green-band emission (vacancy oxygen-related PL emission in ZnO) centered at about 516 nm after annealing the ZHDS nano-sheets at 400^{o}C for 3 hours. We confirmed that the -OH groups in the crystal structures should play the main role for the strong blue-band emission originated from ZHDS. The obtained ZHDS with excellent fluorescence emission would greatly benefit the rational design of high-performance metallo/ organic compounds for low-cost light emitting devices. By using laser ablation in liquid, our results prove a novel strategy to conjugation of metal complexes and organic structures directly from bulk targets with surfactants as templates. The low-cost, convenient and direct synthesis will be very suitable for developing various metallo/organic functional materials.

Acknowledgements

This work was supported by the Natural Science Foundation of China under Grant Nos.11105085, 11275116 and 11375108, the Fundamental Research Funds of Shandong University under Grant No. 2015JC007, the Excellent Youth and Middle Age Scientists Fund of Shandong Province under Grant No. BS2012CL024.

References:

1 P. Sista, K. Ghosh, J. S. Martinez and R. C. Rocha, *Polymer Reviews,* 2014, **54**, 627-676.

2 F. Wang, J. H. Seo, Z. Q. Ma and X. D.Wang, *ACS Nano*, 2012, **6**, 2602-2609.

3 F. Wang, J. E. Jakes, D. L. Geng and X. D.Wang, *ACS Nano*, 2013*,* **7**, 6007-60016.

4 O. Altuntasoglu, Y. Matsuda, S. Ida and Y. Matsumoto, *Chem. Mater*., 2010, **22**, 3158-3164.

5 C. Liang, Y. Shimizu, M. Masuda, T. Sasaki and N. Koshizaki, *Chem. Mater.*, 2004, **16**, 963-965.

6 T. Yu, B. Lim and Y. N. Xia, *Angew. Chem. Int. Ed.*, 2010, **49**, 4484-4487.

7 J. W. Seo, Y. W. Jun, S. W. Park, H. Nah, T. Moon, B. Park, J. G. Kim, Y. J. Kim and J. Cheon, *Angew. Chem. Int. Ed.*, 2007, **46**, 8828-8831.

8 Y. Hernandez, V. Nicolosi, M. Lotya, F. M. Blighe, Z. Sun, S. De, I. T. McGovern, B. Holland, M. Byrne, Y. K. GunKo, J. J. Boland, P. Niraj, G. Duesberg, S. Krishnamurthy, R. Goodhue, J. Hutchison, V. Scardci, A. C. Ferrari and J. N. Coleman, *Nat. Nanotechnol*., 2008.3, 563

9 S. kim, J. Wu, A. C. Carlson, S. H. Jin, A. Kovalsky, P. Glass, Z. J. Liu, N. Ahmed, S. L. Elgan, W. Q. Chen, P. M. Ferreira, M. Sitti, Y. Q. Huang and J. A. Rogers, *Proc. Natl. acad. Sci. U.S.A*, 2010, **107**, 17095-17100.

10 H. C. Ko, A. J. Baca and J. A. Rogers, *Nano Lett.*, 2006, **6**, 2318–2324.

11 J.Yoon, S. Jo, I. S. Chun, I. Jung, H. S. Kim, M. Meitl, E. Menard, X. L. Li, J. J. Coleman, U. Paik and J.A. Rogers, *Nature*, 2010, **465**, 329–330.

12 Z. J. Yan, R. Q. Bao and D. B. Chrisey, *Langmuir*, 2011, **27(2)**, 851–855.

13 S. Li, M. Chen and X. D. Liu, *Opt. Express*, 2014, **22(15)**, 18707–18714.

14 M. Chen, X. D. Liu, Y. H. Liu and M. W. Zhao, *J. Appl. Phys.* 2012, **111**, 103108(1)–103108(4).

15 C. Liang, Z. Tian, T. Tsuruoka, W. Cai and N. Koshizaki, *J. Photoch. Photobio.A.*2011, **224(1)**, 110-115.

16 H. Y. Liu, H. Wu, J. F. Ma, J. Yang and Y. Y. Liu, *Dalton Trans.*, 2009, **38**, 957–7968.

17 W. I. Lee, Y. Bae and A. J. Bard, *J. Am. Chem. Soc.*, 2004, **126**, 8358 -8359.

18 X. L. Wu, S. J. Xiong, J. Zhu, J. Wang, J. C. Shen and P. K. Chu, *Nano Lett.*, 2009, 9, 4053-4060.

19 F. Luo, M. S.Wang, M. B. Luo, G. M. Sun, Y. M. Song, P. X. Li and G. C. Guo, *Chem. Commun.*, 2012, **48**, 5989–5991.

20 R. E. Hummel, M. H. Ludwig, J. Hack and S.-S. Chang, *Solid. State. Commun.* 1995, **96**, 683-687.

21 G. Mandal, S. Bhattacharya and T. Ganguly, *Chem. Phys. Lett.*, 2009, **478**, 271–276.

22 N. Goswami and D. K. Sharma, *Physica. E.*, 2010, **42**, 1675–1682.

23 M. H. Jung and M. J. Chu, *Nanoscale.*, 2014, **6**, 9241–9249.

24 Y. S. Fu, X. W. Du, S. A. Kulinich, J. S. Qiu, W. J. Qin, R. Li, J. Sun and J. Liu, *J. Am. Chen. Soc.* 2007, **129**, 16029–16033.